Journal of Chemical and Petroleum Engineering (JChPE)

Print ISSN: 2423-673X Online ISSN: 2423-6721

Preparation of Activated Carbon from Entada Africana Guill. & Perr for CO_2 Capture: Artificial Neural Network and Isotherm Modeling

Zohreh Khoshraftar, Ahad Ghaemi *

1. School of Chemical, Petroleum and Gas Engineering, Iran University of Science and Technology, Tehran, Iran. E-mail: zohreh_khoshraftar@mail.iust.ac.ir
2. School of Chemical, Petroleum and Gas Engineering, Iran University of Science and Technology, Tehran, Iran. E-mail: aghaemi@iust.ac.ir

ARTICLE INFO

Article History:
Received: 02 April 2022
Revised: 20 April 2022
Accepted: 23 April 2022

Article type: Research

Keywords:
Activated Carbon,
ANN,
CO_2 Adsorption,
Entada Africana Guill. & Perr,
Isotherm Model

ABSTRACT

Recent concerns about the greenhouse effect and climate change have been prominent worldwide. In this study, a single-step KOH activation was used to prepare Entada porous carbon adsorbent. The produced activated carbon was used for CO_2 adsorption. Isotherm models including Freundlich, Langmuir, Dubinin-Rudeshkovich, Temkin, and Hill were used for adsorption isotherm data. In addition, artificial neural networks were used for the prediction of CO_2 adsorption capacity. Trial and error helped us to find the best design, selecting the architecture with the lowest error (MSE) and the best regression coefficient. The best MSE validation performance of the neural network was 0.00094486. The neural network model can effectively predict CO_2 adsorption on activated carbon from Entada Africana Guill. & Perr. Adsorption capacities of activated carbon from Entada Africana Guill. & Perr at 273 k and 289 k and 1 bar were 4.34 mmol/g and 6.78 mmol/g, respectively. The Brunauer–Emmett–Teller specific area (S_{BET}) and the micropores volume equated to 2556 m^2/g and 0.78 cm^3/g, respectively. Thus, Entada African Guill & Perr activated carbon shows promise in capturing CO_2.

Introduction

At present, atmospheric CO_2 is at 410 ppm, which is 46.4% higher than preindustrial levels. For a long time in the future, the trend toward increasing energy use will continue to grow due to fossil fuels, which will continue to be the most crucial source of human energy demand [1]. It is vital to develop technology that can capture CO_2 efficiently as CO_2 concentrations in the atmosphere rise [2, 3]. The capture and storage of CO_2 after the combustion of fossil fuels is a practical and important solution for mitigating the ever-increasing CO_2 emissions from fossil fuel consumption [4]. Various technologies for carbon dioxide removal have been proposed, among which adsorption is suitable [5]. In recent decades, the adsorption technique concerned significant attention in the view of environmental preservation and generating clean energy [6, 7]. Among various methods, the alternative that has concerned significant attention is adsorption using highly porous materials, which show numerous advantages as CO_2 adsorbents, such as low energy consumption [8]. An ideal CO_2 adsorbent can adsorb high CO_2 concentrations, has excellent recyclability, can easily be regenerated, has a high CO_2

* Corresponding Author: A. Ghaemi (E-mail address: aghaemi@iust.ac.ir)

Journal of Chemical and Petroleum Engineering, 2022, 56(1): 165- 180.
Publisher: University of Tehran, College of Engineering *DOI: 10.22059/JCHPE.2022.341031.1387*

selectivity, is low cost, and has fast adsorption kinetics process [4, 9]. Solid adsorbents that selectively adsorb carbon dioxide at ambient temperature and pressure (25 °C, 1 bar) could offer a competitive alternative to amine-based solvents, such as porous polymers, porous carbons [7, 10, 11], metal-organic frameworks (MOFs) [12–19], graphene [20], and zeolites[21–27]. Carbon porous materials exhibit high specific surface area and pore volume, good thermal and chemical stability, and easy pore-structure adjustment [10]. To prepare highly porous carbon, KOH is one of the main activators. Wang et al. developed a cost-effective CO_2 adsorbent using activated rice husk carbon based on KOH (KOH-AC, 1439 m^2/g). The adsorption rate of rice husk-based activated carbon under indoor conditions at a low concentration of CO_2 (2000 ppm ~ 500 ppm) was 2.1 mmol/g [1]. A combination of hydrothermal treatment and mild KOH activation is used by Wang et al. to prepare carbon using chitosan as a precursor. The carbon activated by KOH at 600 °C obtained from the salt-assisted hydrochar exhibited the highest CO_2 uptake (4.41 mmol/g), despite its surface area of 1249 m^2/g. This indicates that the amount of CO_2 adsorbed in carbon is determined both by its microporosity and its active N-types [28]. In the first step of converting garlic peel into hydrochar, KOH was used by Huang et al. to achieve high surface areas and large pores in the activated carbons. Activated carbon prepared by KOH at 800 °C with a KOH/hydrochar ratio of 2 exhibits good pore structure with a surface area of 1262 m^2/g [29]. Li et al. made biochars containing 70% pine sawdust and 30% sewage sludge through KOH modification to investigate CO_2 adsorption behavior. Compared to pristine biochars (35.5–42.9 mg/g), modified biochars had higher CO_2 adsorption capacities of 136.7–182.0 mg/g [30].

ANN is a nonlinear statistical model tool developed in the 1980s, and also using this tool rapidly are gaining popularity today. The process allows for modeling inputs and outputs in complex nonlinear systems, and it is an efficient tool for modeling these processes [31]. Models used to discuss the adsorption process should satisfy certain conditions to identify the relationship between variables, such as the dependence of calculated parameters on the adsorption mechanism. ANN, which can perform mathematical functions for linear and nonlinear systems, is thus an excellent tool for this approach [32]. ANN predicts an output based on an input using a learning method. ANN is similar to the human brain in that it can mimic its functions while learning [33]. A first-of-its-kind adsorbent was made from Entada Africana Guill & Perr in the present study to adsorb carbon dioxide. It is the first study involving active carbon from Entada Africana Guill & Perr for CO_2 adsorption through KOH impregnation. Therefore, the objective of this study is to investigate the performance of activated carbon from Entada Africana Guill. & Perr, as a cheap and efficient adsorbent, for CO_2 adsorption. Detailed characterization of the AC is presented here, as is an analysis of CO_2 adsorption at 273 and 298 K. The properties of activated carbon prepared by chemical activation with KOH have been characterized using Brunauer-Emmett-Teller (BET), Fourier transforms infrared (FTIR), and scanning electron microscopy (SEM). During the investigation, Freundlich, Langmuir, Dubinin-Radushkevich (DR), Hill, and Temkin isotherm models were used for adsorption process modeling. Ultimately, the ANN model was used for estimation of CO_2 adsorption capacity.

Experimental

Porous Carbon Synthesis

Entada Africana Guill. & Perr was collected from forests of northern Iran (Anzali). KOH is used for chemically activating biomass to produce activated carbon. The most effective and commonly used activator is KOH, as it can create a high total pore volume (especially

micropores) and a large specific surface area [1]. For 24 hr, the drying process was conducted at 100 °C to remove any moisture from the biomass. The powder of the sample was obtained by crushing. Activation and carbonization were applied in a one-step process. An aqueous solution containing KOH was immersed in the precursor for 3 hr. A 1:2 impregnation ratio was used to mix biomass with KOH. After 24 hr of heating at 100°C, the mixture was cooled. After being dried for 24 hr at 100 °C, the mixtures were activated for 60 min in a pure N_2 flow at 800 °C. Once the activated carbon had been washed three times with distilled water, it was immersed in 1 M HCl, then again in water to remove the chloride ions, then finally allowed to air dry. In the final step, AC was dried at 100 °C for 12 hr [34]. The preparation of activated carbon steps has been indicated in Fig. 1.

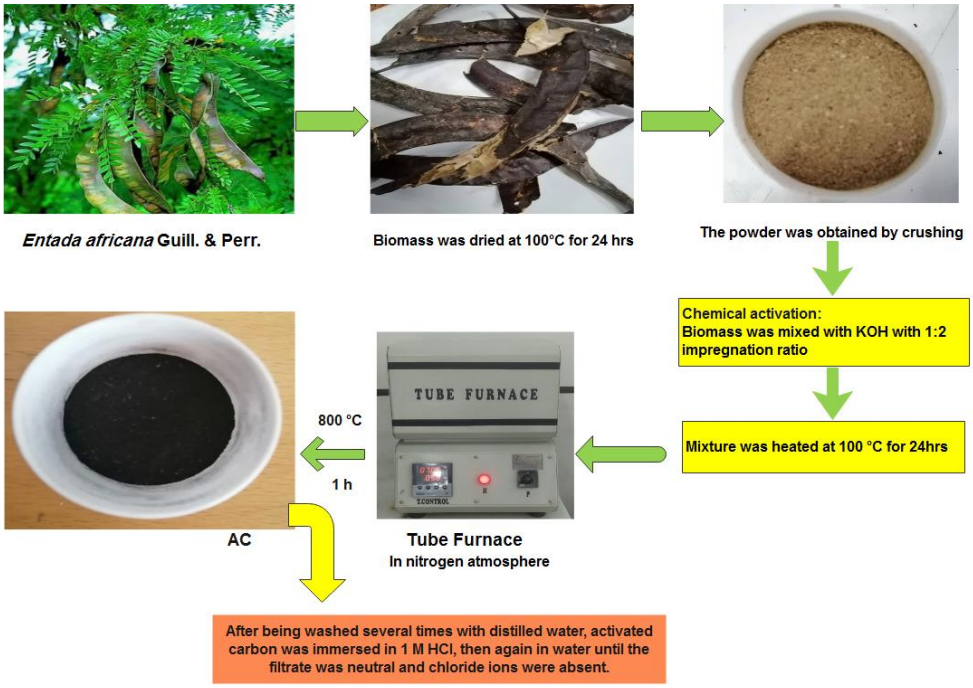

Fig. 1. The preparation steps of AC

Gas Adsorption

Activated carbon from Entada Africana Guill. & Perr was tested to determine its CO_2 adsorption capacity using a cylindrical reactor shown in Fig. 2 A stainless steel reactor with a cylindrical shape and a grid cell for exposing the CO_2 sample is available. The AC is inserted into the cylindrical enclosure of the device and completely sealed. A total of 0.5 g of the synthesized porous carbon was loaded into the fully sealed cylindrical reactor. As a measurement of the amount of gas absorbed, pure CO_2 is injected into the chamber for 60 min at a temperature of 0 °C and 25°C and a pressure of 0-1 bar. A pressure gauge and regulator were used to reach the desired pressure and then enter the mixing chamber with the CO_2 from the high-quality cylinder. In addition to the electrical heat trace, a computer records the temperature and pressure of the reactor in real-time.

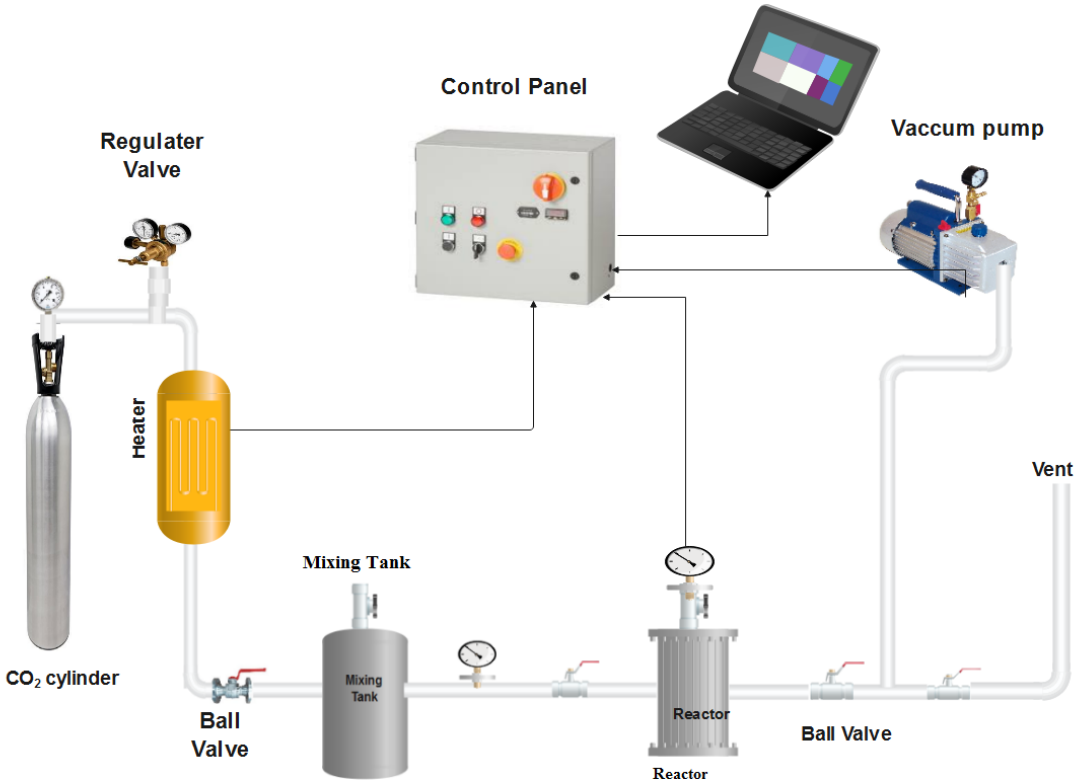

Fig. 2. A schematic of the experimental set up for CO_2 adsorption

Eq. 1 is used to determine adsorption capacity of the activated carbon.

$$q = \frac{m_i - m_f}{w} = \left(\frac{VM_w}{Rw}\right)\left(\frac{P_i}{Z_i T_i} - \frac{P_f}{Z_f T_f}\right) \tag{1}$$

$$Z = 1 + \frac{BP}{RT} \tag{2}$$

An initial and final condition is indicated by the subscripts *i* and *f*. Pressure, temperature, reactor volume, universal gas constants, compressibility factor, and Entada Africana Guill. & Perr adsorbent mass is symbolized by the constants of *P*, *V*, *R*, *Z*, and *w*, respectively. Virial equation (eq.2) was used for the calculation of the compressibility factor [35].

Characterization

A micrometric ASAP 2020 instrument recorded the pore structure of porous carbon. In preparation for adsorption-desorption analyses, samples were degassed to constant weight under dynamic vacuum conditions for 2 hr at 393K. A scanning electron microscope (SEM) [model: TESCAN Vega 3] is used to analyze the structure and morphology of activated carbon. A Perkin Elmer FT-IR spectrometer was used to detect functional groups on AC surfaces.

ANN Model

The neural network is based on the concept of mimicking the actual human nervous system, which is a complex, parallel, and nonlinear method of processing information. The artificial neurons are interconnected in a network architecture based on specific specifications. A neural network (ANN) is a technique that creates meaningful outputs from inputs using a series of

three layers (Input layer, hidden layer, and output layer). Input layers receive data, which is then processed by the hidden layers, which pass it on to the output layer. Neurons process every data record according to a specific activation function, such as sigmoid, tanh, linear, etc. [36]. Every connection has a corresponding weight value. In the hidden layer, the neurons in the final layer produce the following output [33]:

$$h_i = \sigma(\sum_{j=1}^{N} W_{ij} x_j + T_i^{hid}) \tag{3}$$

where the activation function is defined as σ, N is the number of input neurons, the weights are W, the inputs of the input neurons are x_j, and the threshold terms of the hidden neurons are T^{hid}.

The adsorption parameters of CO_2 using activated carbon from Entada Africana Guill. & Perr was modeled by a feed-forward radial base function (RBF), with a 2:10:1 architecture, as illustrated in Fig. 3. The numbers from the 38 data (70 % training) were used for the training sample and 16 data for the network calculation [15% validation: 8 samples and 15% testing: 8 samples]. As the Tan-Sigmoid transfer function (tansig) was applied as an activation function for the hidden layer neurons. Additionally, the present study included the input variables pressure and temperature. Adsorption on the AC produced an output variable or process response (The amount of CO_2 adsorbed). The optimal hidden layer of the ANN model using different architectures with 2 to 20 neurons was obtained. ANN is trained using the mean square errors (MSE) statistical parameter. As shown in Fig. 4, the calculated MSE values are plotted against the number of neurons in the hidden layer. Specifically, ten neurons in the middle layer were selected to gain the minimum error. The MSE and correlation coefficient (R^2) were calculated using Eq. 4 and Eq. 5, respectively [37].

$$MSE = \frac{1}{N} \sum_{i=1}^{N} (Y_{predicted} - Y_{real})^2 \tag{4}$$

$$R^2 = \sum_{i=1}^{N} \frac{(Y_{predicted} - Y_{real})^2}{(Y_{predicted} - Y_{mean})^2} \tag{5}$$

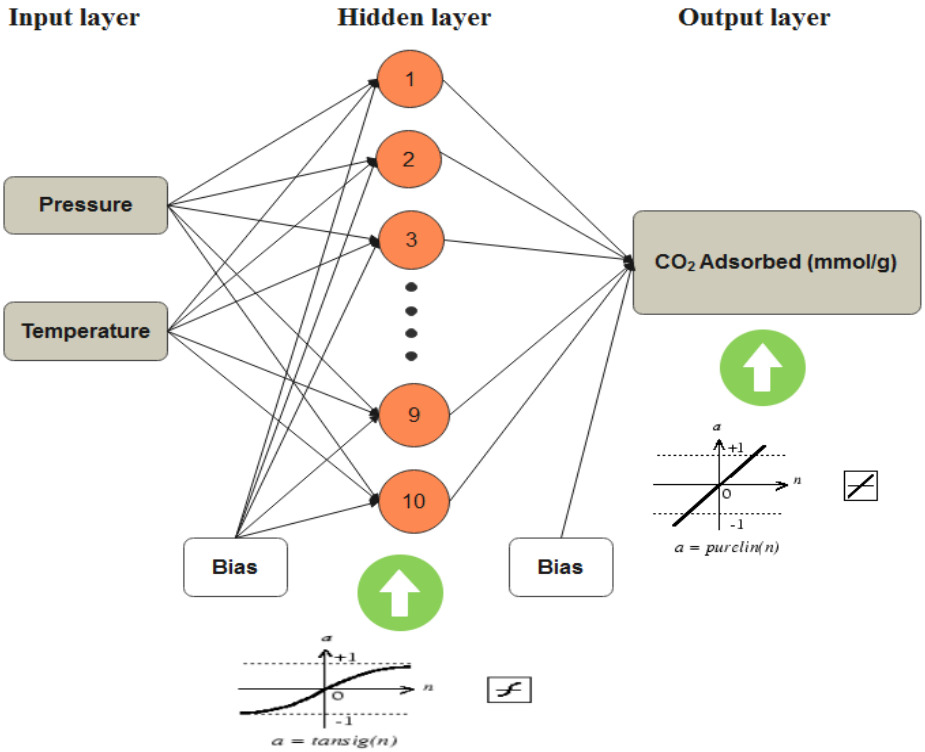

Fig. 3. RBF was applied to optimize CO_2 adsorption on activated carbon from Entada Africana Guill. & Perr

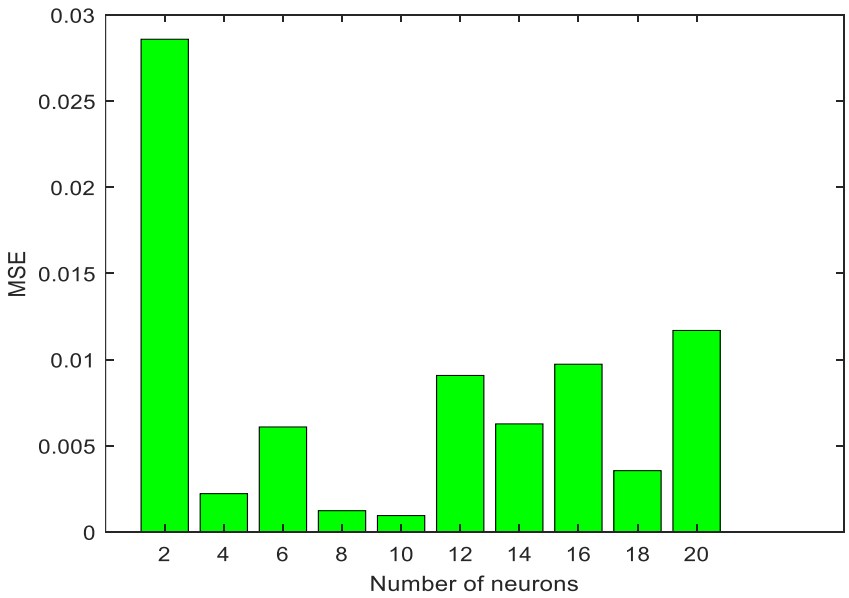

Fig. 4. Values of mean square errors versus the number of neurons

Results and Discussion

Gas adsorption experiments were carried out on activated carbon from Entada Africana Guill. & Perr at STP up to a relative pressure (P/P_0) of 1.0. Fig. 5 demonstrates the stepwise uptake of nitrogen at 77 K. The curve demonstrated a second sharp rise up to 0.85 bar after a steep rise of 500 cm^3/g at low relative pressures ($P/P_0 < 0.02$). The curve then gradually

increased up to 1 bar. Based on these observations, the material was characterized by micropores, which were visible in the pattern of the pore size distribution (Fig. 6). It appears that the large voids trap gas, causing a mild hysteresis between absorption and desorption. Consequently, the S_{BET} and the micropores volume equated to 2556 m^2/g and 0.78 cm^3/g, respectively. The value of this material surpasses most porous carbon types.

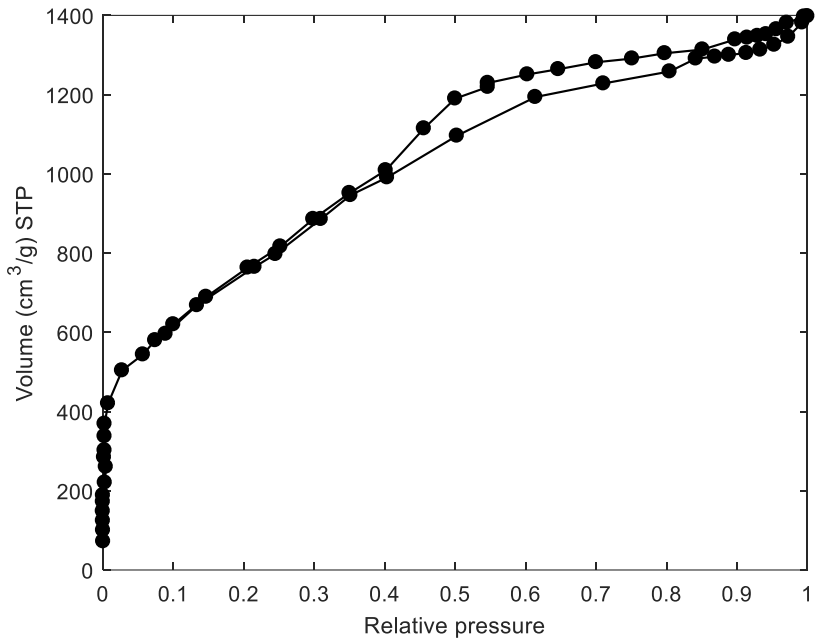

Fig. 5. N_2 adsorption–desorption of the activated carbon

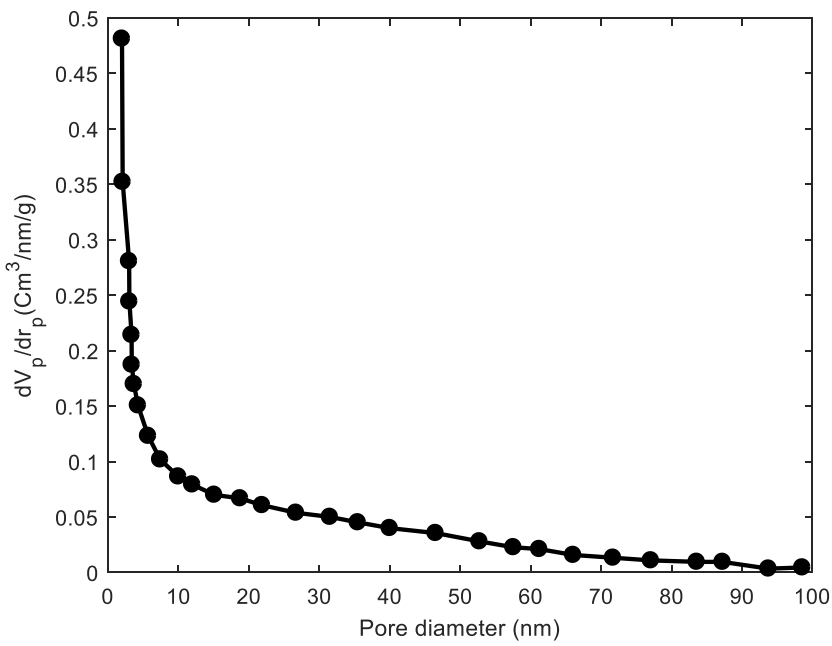

Fig. 6. Distribution curves of pore sizes for BJH

Activated carbon from Entada Africana Guill. & Perr was examined using a scanning electron microscope (SEM) at 25 kV. As can be seen from the SEM image (Fig. 7), AC is typically composed of a somewhat smooth structure, with irregular pores on the surface.

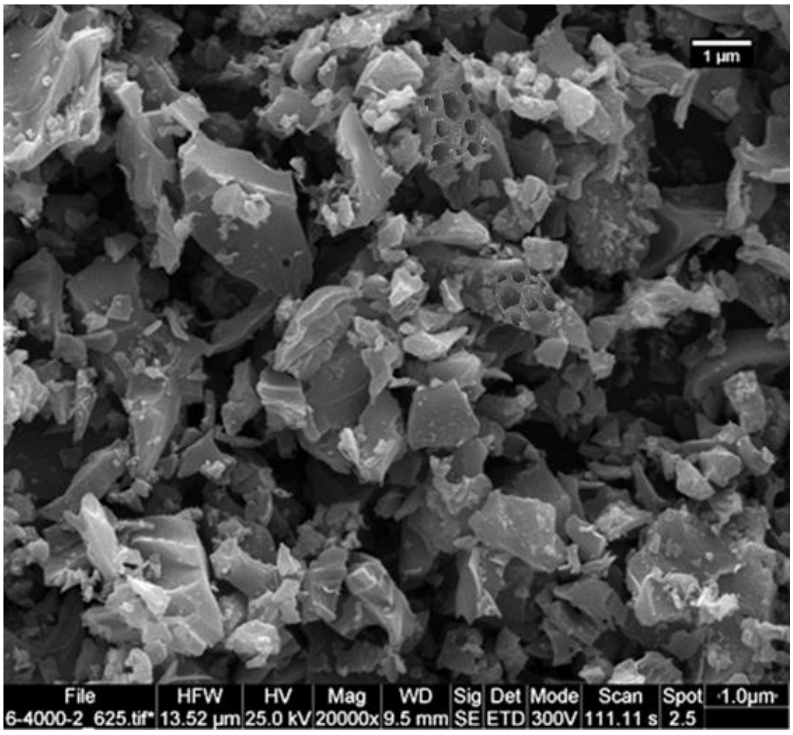

Fig. 7. A scanning electron microscope of activated carbon from Entada Africana Guill. & Perr

The FTIR spectrum of the adsorbent is important for evaluating the presence of the desired functional groups and bonds. From Fig. 8, the FTIR spectrum of Entada Africana Guill. & Perr activated carbon can be seen. –OH stretching of hydroxyl groups is responsible for the peak at 3430 cm^{-1}. Molecular vibrations of methoxyl groups are seen at 2924 cm^{-1}, which corresponds to symmetric and asymmetric vibrations of C–H. A peak at 1057 cm^{-1} is attributed to vibrations from the C–O [34].

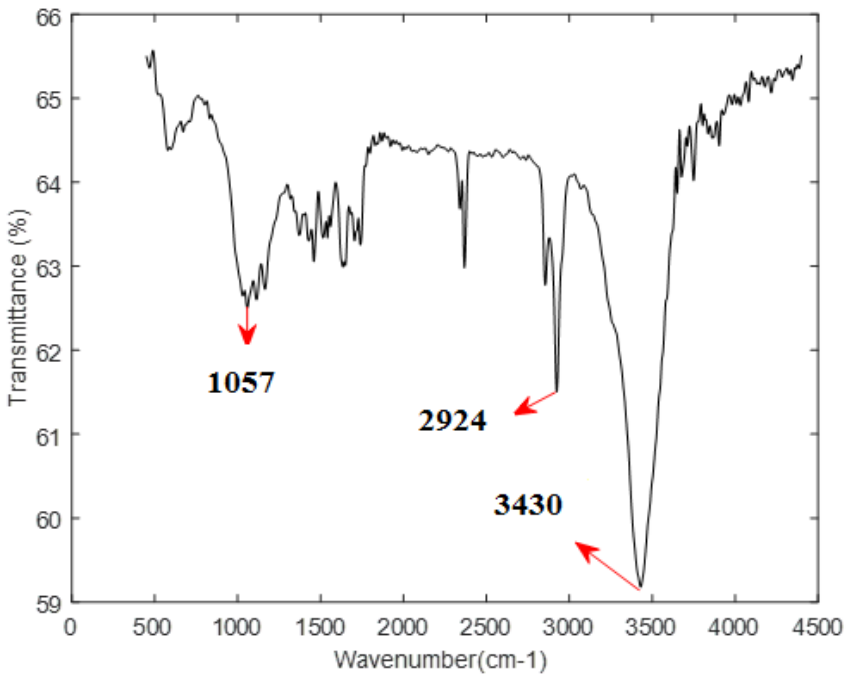

Fig. 8. FTIR spectrum of activated carbon from Entada Africana Guill. & Perr

Modeling of CO_2 Adsorption by ANN

The adsorption capacity is predicted using the Neural Network Toolbox from MATLAB 2017a. In the current study, the artificial neural network consisted of two inputs, one hidden layer with ten neurons within it, and one target output. The best design was found through trial and error, selecting the architecture with the lowest error (MSE) and the best correlation coefficient. Experimental results and neural network model output values (CO_2 adsorbed) are shown in Fig 9. Results show that for the whole set of data, the linear coefficient of determination was 0.9998. ANN model can effectively predict CO_2 adsorption on activated carbon from Entada Africana Guill. & Perr from the modeling data. Based on the performance graph, the network achieves the highest level of validation (Fig 10). Based on the optimized weight of the CO_2 adsorption network, Table A1 displays the results of the ANN model for predicting ANN weights [38].

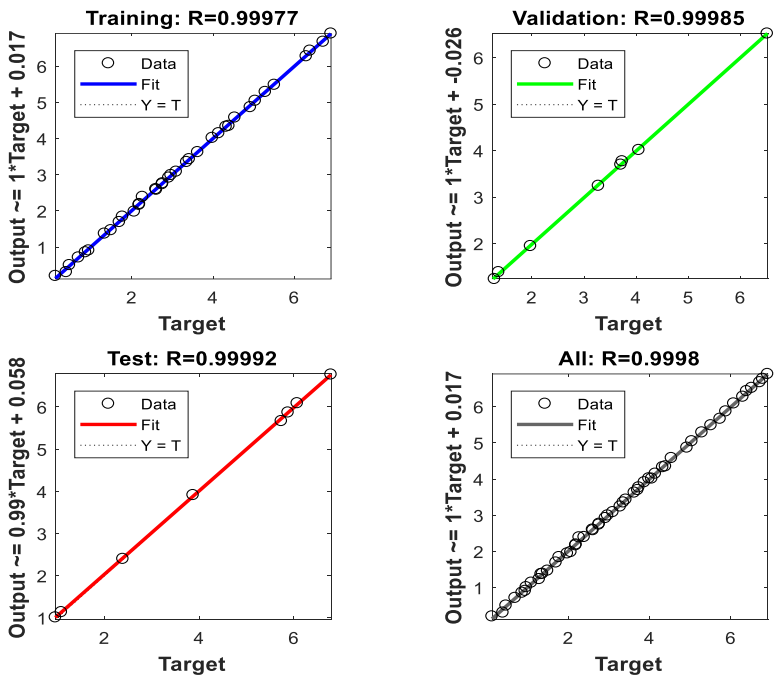

Fig. 9. ANN regression data for training, test and validation steps

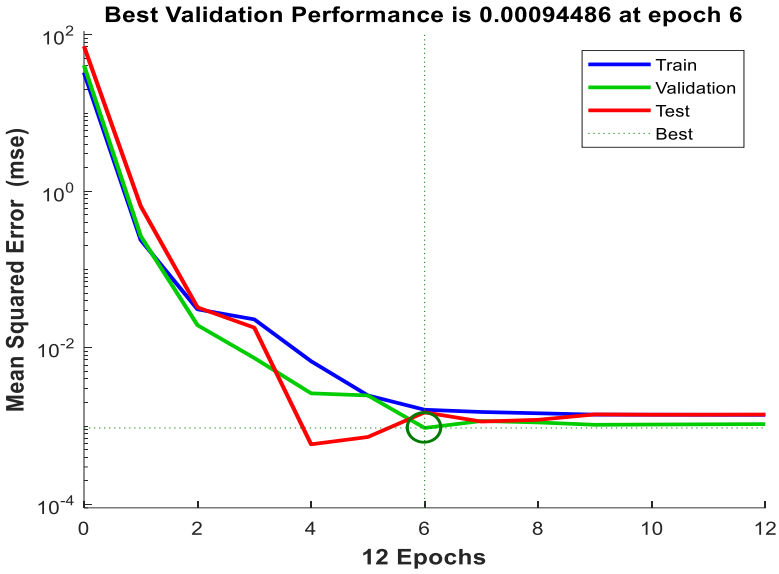

Fig. 10. The validation performance of the best ANN

The Effect of Temperature and Pressure

An adsorption isotherm of CO_2 at 273 K and 298 K is shown in Fig. 11. The isotherm has a significant impact on the uptake of carbon dioxide by the activated carbon based on Entada Africana Guill. & Perr. Fig. 11illustrates how the amount of CO_2 that can adsorbates decreases as the adsorption temperature increases. The amount of adsorption increases with increasing pressure, because adsorption is exothermic, it decreases as temperature increases. CO_2 adsorption by several activated carbons was compared (Table 1). Comparing the measured CO_2 adsorption capacity to that reported in other studies show that the current activated carbon from Entada Africana Guill. & Perr almost the same performs as the others and indicates the excellent CO_2 adsorption at 273 K and 298 K. The results of this research can be used to develop a new activated carbon from Entada Africana Guill. & Perr that is effective for CO_2 uptake.

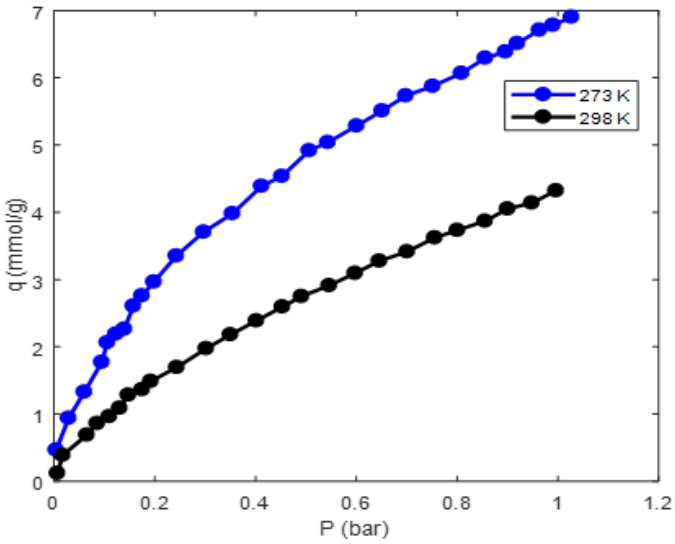

Fig. 11. Adsorption of CO_2 at 273 K and 298 K under pressure of 0–1 bar using the activated carbon from Entada Africana Guill. & Perr

Table 1. Comparison of CO_2 adsorption capacity of Entada Africana Guill. & Perr AC and other activated carbons

Precursor	Activation temperature (K)	Activation Time (hr)	Adsorption temperature(°C)	BET (m2/g)	Adsorption (mmol/g)	Ref.
Coffee grounds	673	1	0 25	840	4.7 3.0	[39]
Celtuce leaves	800	1	0 25	3404	6.0 4.4	[40]
Granular Bamboo	973	1.5	0 25	1846	7.0 4.7	[41]
Sawdust	600	1	0 25 50	1260	6.1 4.8 3.6	[42]
Garlic peel	600	1	25	947	4.2	[29]
Date Sheets	800	1	0 25	2367	6.4 4.3	[43]
Entada africana Guill. & Perr	800	1	0 25	2556	6.8 4.3	This study

Isotherm Modeling

CO_2 adsorption rate is a function of gas pressure. The adsorption profile of CO_2 at 273 K and 298 K and ambient pressure is illustrated in Fig. 12. According to Fig. 12, CO_2 adsorption capacity decreases with increasing temperature, which can be explained by the lower binding strengths of the CO_2 adsorbate and the Entada Africana Guill. & Perr activated carbon [44]. Additionally, at elevated temperature, the CO_2 adsorption capacity reduces which determines that the sorption process is exothermic, defining an occurrence of physical sorption. Physisorption, as opposed to chemisorption, is mediated by a weak van der Waals force, which tends to be broken as temperature increases, decreasing adsorption capacity [44, 45]. According to the regression method, Table 2 predicts the isotherm constants and corresponding R^2 values for the CO_2 adsorption.

Based on the R^2 values in Table 2, Hill isotherm is the best fit for the adsorbent at 273 K (Fig. 12). Table 2 shows that Freundlich and Hill isotherms (Fig. 12) are the best-fit models for the adsorbent of activated carbon from Entada Africana Guill. & Perr at 298 K based on R^2 values. The Freundlich model implies that CO_2 adsorption is multilayer and not restricted to a monolayer on the activated carbon surface [44]. The Hill model is usually applied to explain the binding of different species on homogeneous substrates [46]. At elevated temperatures, endothermic desorption is more advantageous, thus reducing CO_2 adsorption capacity. The Freundlich constant, n, in Table 2, concludes that the CO_2 adsorption will be favorable. As well as providing useful information regarding energy parameters, in terms of E (mean free energy of adsorption) and A_T (heat of adsorption), the Dubinin Radushkevich and Temkin isotherms are also helpful. Energy parameter values of 3 and 4 kJ/mol show that the CO_2 adsorption process is purely physical [47].

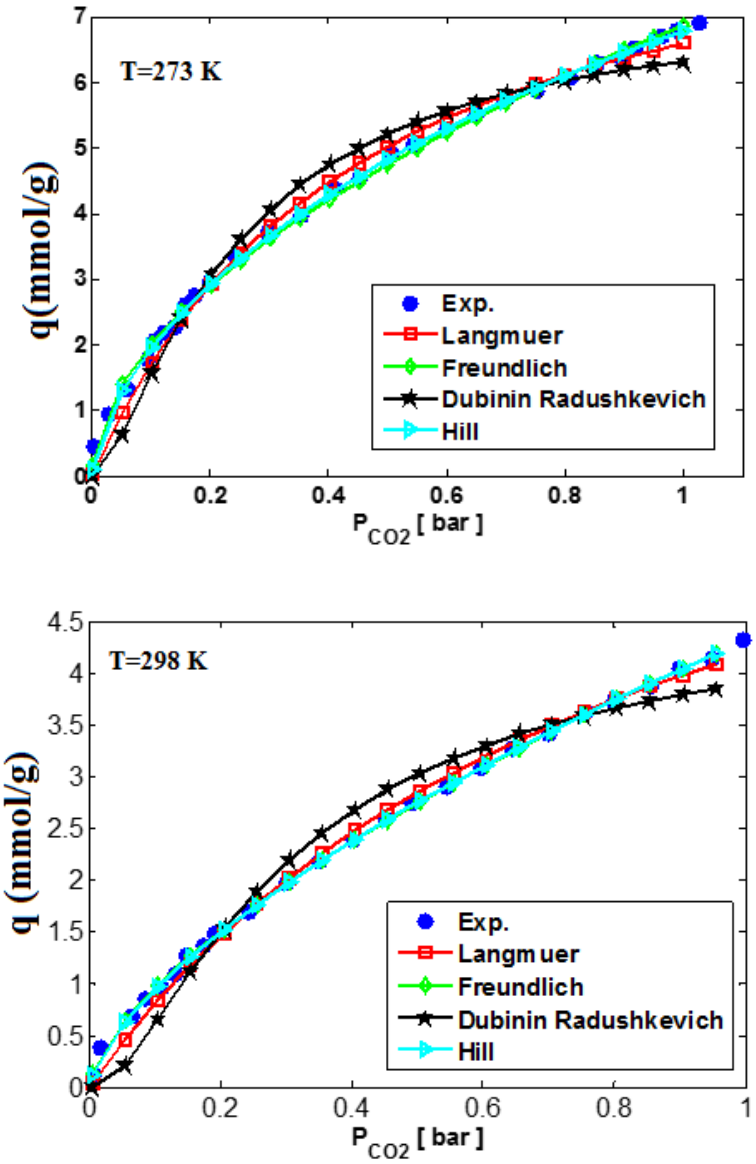

Fig. 12. Experimental data and isotherm models at 273 K and 298 K for CO_2 adsorption

Table 2. Isotherm modeling parameters for CO_2 adsorption

n	Parameters	Unit	273 K		298 K	
			Value	R^2	Value	R^2
Langmuir	q_m	mmol g^{-1}	9.617	0.997	7.806	0.998
	K_L	L/mg	2.181		1.151	
Freundlich	n	n	1.882	0.998	1.526	0.999
	K_F(mg/g)	mmol g^{-1}. $bar^{-1})^{1/n}$	6.865		4.326	
Temkin	B		1.453	0.929	0.933	0.917
	A_T	L mol^{-1}	61.404		44.827	
Dubinin-Rudeshkovich	E	kJ mol^{-1}	3.114	0.987	2.965	0.985
	β	$mol^2.KJ^{-2}$	0.052		0.057	
	q_m	mmol g^{-1}	7.188		4.606	
Hill	q_s	mmol/L	23.856	0.999	72.349	0.999
	n	$mg^{(1-m)}$. L^m/g	0.648		0.679	
	K_D	$(L/mg)^m$	2.517		15.776	

Conclusion

A biomass-derived carbon was successfully activated and carbonized by KOH to achieve high CO_2 adsorption capacity. The activation was performed over 800 °C at a holding time of 60 min. The structure and properties of AC have been characterized using scanning electron microscopy (SEM), Fourier transform infrared (FTIR), and Brunauer-Emmett-Teller (BET). The specific surface area (S_{BET}) was 2556 m^2/g, and the total pore volume equaled 0.78 cm^3/g. This carbon demonstrates high CO_2 uptake of 6.78 mmol/g at 0°C and 1 bar. The CO_2 adsorption capacity decreases with increasing temperature, which can be explained by lower binding strengths between the adsorbate and the activated carbon. The adsorption capacity of AC-KOH at 289 k and 1 bar was 4.34 mmol/g. Freundlich and Hill isotherms are the best-fit models for the adsorbent of the activated carbon at 298 K based on R^2 values. Hill isotherm is the best-fit model for the adsorbent at 298 K. Results show that for the whole set of data the linear correlation coefficient was 0.9998. The ANN results showed that the neural network model can effectively predict CO_2 adsorption on the activated carbon. Based on the results of the models, they were quite successful in predicting process performance.

References

[1] Wang S, Lee YR, Won Y, Kim H, Jeong SE, Hwang BW, Cho AR, Kim JY, Park YC, Nam H, Lee DH. Development of high-performance adsorbent using KOH-impregnated rice husk-based activated carbon for indoor CO_2 adsorption. Chemical Engineering Journal. 2022 Feb 21:135378.

[2] Khoshraftar Z, Ghaemi A. Presence of activated carbon particles from waste walnut shell as a biosorbent in monoethanolamine (MEA) solution to enhance carbon dioxide absorption. Heliyon. 2022 Jan 1;8(1):e08689.

[3] Khoshraftar Z, Ghaemi A, Mohseni Sigaroodi AH. The effect of solid adsorbents in Triethanolamine (TEA) solution for enhanced CO_2 absorption rate. Research on Chemical Intermediates. 2021 Oct;47(10):4349-68.

[4] Cui H, Xu J, Shi J, You S, Zhang C, Yan N, Liu Y, Chen G. Evaluation of different potassium salts as activators for hierarchically porous carbons and their applications in CO_2 adsorption. Journal of Colloid and Interface Science. 2021 Feb 1;583:40-9.

[5] Pashaei H, Ghaemi A. Review of CO_2 capture using absorption and adsorption technologies. Iranian Journal of Chemistry and Chemical Engineering (IJCCE). 2021 Nov 28.

[6] Karimi M, Shirzad M, Silva JA, Rodrigues AE. Biomass/Biochar carbon materials for CO_2 capture and sequestration by cyclic adsorption processes: A review and prospects for future directions. Journal of CO2 Utilization. 2022 Mar 1;57:101890.

[7] Yang C, Zhao T, Pan H, Liu F, Cao J, Lin Q. Facile preparation of N-doped porous carbon from chitosan and NaNH2 for CO_2 adsorption and conversion. Chemical Engineering Journal. 2022 Mar 15;432:134347.

[8] Serafin J, Ouzzine M, Cruz Jr OF, Sreńscek-Nazzal J, Gómez IC, Azar FZ, Mafull CA, Hotza D, Rambo CR. Conversion of fruit waste-derived biomass to highly microporous activated carbon for enhanced CO_2 capture. Waste Management. 2021 Dec 1;136:273-82.

[9] Oschatz M, Antonietti M. A search for selectivity to enable CO_2 capture with porous adsorbents. Energy & Environmental Science. 2018;11(1):57-70.

[10] Jin C, Sun J, Chen Y, Guo Y, Han D, Wang R, Zhao C. Sawdust wastes-derived porous carbons for CO_2 adsorption. Part 1. Optimization preparation via orthogonal experiment. Separation and Purification Technology. 2021 Dec 1;276:119270.

[11] Ma C, Lu T, Shao J, Huang J, Hu X, Wang L. Biomass derived nitrogen and sulfur co-doped porous carbons for efficient CO_2 adsorption. Separation and Purification Technology. 2022 Jan 15;281:119899.

[12] Al-Rowaili FN, Zahid U, Onaizi S, Khaled M, Jamal A, AL-Mutairi EM. A review for Metal-Organic Frameworks (MOFs) utilization in capture and conversion of carbon dioxide into valuable products. Journal of CO_2 Utilization. 2021 Nov 1;53:101715.

[13] Gaikwad S, Kim Y, Gaikwad R, Han S. Enhanced CO_2 capture capacity of amine-functionalized MOF-177 metal organic framework. Journal of Environmental Chemical Engineering. 2021 Aug 1;9(4):105523.

[14] Younas M, Rezakazemi M, Daud M, Wazir MB, Ahmad S, Ullah N, Ramakrishna S. Recent progress and remaining challenges in post-combustion CO_2 capture using metal-organic frameworks (MOFs). Progress in Energy and Combustion Science. 2020 Sep 1;80:100849.

[15] Du L, Lu Z, Zheng K, Wang J, Zheng X, Pan Y, You X, Bai J. Fine-tuning pore size by shifting coordination sites of ligands and surface polarization of metal–organic frameworks to sharply enhance the selectivity for CO_2. Journal of the American Chemical Society. 2013 Jan 16;135(2):562-5.

[16] Liu M, Nothling MD, Webley PA, Jin J, Fu Q, Qiao GG. High-throughput CO_2 capture using PIM-1@ MOF based thin film composite membranes. Chemical Engineering Journal. 2020 Sep 15;396:125328.

[17] C Trickett CA, Helal A, Al-Maythalony BA, Yamani ZH, Cordova KE, Yaghi OM. The chemistry of metal–organic frameworks for CO_2 capture, regeneration and conversion. Nature Reviews Materials. 2017 Jul 25;2(8):1-6.

[18] Chen W, Zhang Z, Hou L, Yang C, Shen H, Yang K, Wang Z. Metal-organic framework MOF-801/PIM-1 mixed-matrix membranes for enhanced CO_2/N_2 separation performance. Separation and Purification Technology. 2020 Nov 1;250:117198.

[19] Yang DA, Cho HY, Kim J, Yang ST, Ahn WS. CO_2 capture and conversion using Mg-MOF-74 prepared by a sonochemical method. Energy & Environmental Science. 2012;5(4):6465-73.

[20] Ai N, Lou S, Lou F, Xu C, Wang Q, Zeng G. Facile synthesis of macroalgae-derived graphene adsorbents for efficient CO2 capture. Process Safety and Environmental Protection. 2021 Apr 1;148:1048-59.

[21] You HS, Jin H, Mo YH, Park SE. CO_2 adsorption behavior of microwave synthesized zeolite beta. Materials Letters. 2013 Oct 1;108:106-9.

[22] Won W, Lee S, Lee KS. Modeling and parameter estimation for a fixed-bed adsorption process for CO_2 capture using zeolite 13X. Separation and purification technology. 2012 Feb 2;85:120-9.

[23] Wang Y, Du T, Qiu Z, Song Y, Che S, Fang X. CO_2 adsorption on polyethylenimine-modified ZSM-5 zeolite synthesized from rice husk ash. Materials Chemistry and Physics. 2018 Mar 1;207:105-13.

[24] Mortazavi N, Bahadori M, Marandi A, Tangestaninejad S, Moghadam M, Mirkhani V, Mohammadpoor-Baltork I. Enhancement of CO_2 adsorption on natural zeolite, modified clinoptilolite with cations, amines and ionic liquids. Sustainable Chemistry and Pharmacy. 2021 Sep 1;22:100495.

[25] Kareem FA, Shariff AM, Ullah S, Dreisbach F, Keong LK, Mellon N, Garg S. Experimental measurements and modeling of supercritical CO_2 adsorption on 13X and 5A zeolites. Journal of Natural Gas Science and Engineering. 2018 Feb 1;50:115-27.

[26] Dos Santos GC, Bleyer GC, Martins LS, Padoin N, Watzko ES, de Aquino TF, Vasconcelos LB. CO_2 adsorption in a zeolite-based bench scale moving bed prototype: Experimental and theoretical investigation. Chemical Engineering Research and Design. 2021 Jul 1;171:225-36.

[27] De Aquino TF, Estevam ST, Viola VO, Marques CR, Zancan FL, Vasconcelos LB, Riella HG, Pires MJ, Morales-Ospino R, Torres AE, Bastos-Neto M. CO_2 adsorption capacity of zeolites synthesized from coal fly ashes. Fuel. 2020 Sep 15;276:118143.

[28] Wang J, Chen S, Xu JY, Liu LC, Zhou JC, Cai JJ. High-surface-area porous carbons produced by the mild KOH activation of a chitosan hydrochar and their CO_2 capture. New Carbon Materials. 2021 Dec 1;36(6):1081-90.

[29] Huang GG, Liu YF, Wu XX, Cai JJ. Activated carbons prepared by the KOH activation of a hydrochar from garlic peel and their CO_2 adsorption performance. New Carbon Materials. 2019 Jun 1;34(3):247-57.

[30] Li K, Zhang D, Niu X, Guo H, Yu Y, Tang Z, Lin Z, Fu M. Insights into CO_2 adsorption on KOH-activated biochars derived from the mixed sewage sludge and pine sawdust. Science of The Total Environment. 2022 Feb 25:154133.

[31] Yin L, Zheng W, Shi H, Ding D. Ecosystem services assessment and sensitivity analysis based on ANN model and spatial data: A case study in Miaodao Archipelago. Ecological Indicators. 2022 Feb 1;135:108511.

[32] Ghaedi M, Zeinali N, Ghaedi AM, Teimuori M, Tashkhourian J. Artificial neural network-genetic algorithm based optimization for the adsorption of methylene blue and brilliant green from aqueous solution by graphite oxide nanoparticle. Spectrochimica Acta Part A: Molecular and Biomolecular Spectroscopy. 2014 May 5;125:264-77.

[33] Sarkar J, Prottoy ZH, Bari MT, Al Faruque MA. Comparison of ANFIS and ANN modeling for predicting the water absorption behavior of polyurethane treated polyester fabric. Heliyon. 2021 Sep 1;7(9):e08000.

[34] Prakash MO, Raghavendra G, Ojha S, Panchal M. Characterization of porous activated carbon prepared from arhar stalks by single step chemical activation method. Materials Today: Proceedings. 2021 Jan 1;39:1476-81.

[35] Ramezanipour Penchah H, Ghaemi A, Godarziani H. Eco-friendly CO_2 adsorbent by impregnation of diethanolamine in nanoclay montmorillonite. Environmental Science and Pollution Research. 2021 Oct;28(39):55754-70.

[36] Kalam S, Yousuf U, Abu-Khamsin SA, Waheed UB, Khan RA. An ANN model to predict oil recovery from a 5-spot waterflood of a heterogeneous reservoir. Journal of Petroleum Science and Engineering. 2022 Mar 1;210:110012.

[37] Hemmati A, Ghaemi A, Asadollahzadeh M. RSM and ANN modeling of hold up, slip, and characteristic velocities in standard systems using pulsed disc-and-doughnut contactor column. Separation Science and Technology. 2021 Nov 2;56(16):2734-49.

[38] Kolbadinejad S, Mashhadimoslem H, Ghaemi A, Bastos-Neto M. Deep learning analysis of Ar, Xe, Kr, and O_2 adsorption on Activated Carbon and Zeolites using ANN approach. Chemical Engineering and Processing-Process Intensification. 2022 Jan 1;170:108662.

[39] Plaza MG, González AS, Pevida C, Pis JJ, Rubiera F. Valorisation of spent coffee grounds as CO_2 adsorbents for postcombustion capture applications. Applied Energy. 2012 Nov 1;99:272-9.

[40] Wang R, Wang P, Yan X, Lang J, Peng C, Xue Q. Promising porous carbon derived from celtuce leaves with outstanding supercapacitance and CO_2 capture performance. ACS applied materials & interfaces. 2012 Nov 28;4(11):5800-6.

[41] Wei H, Deng S, Hu B, Chen Z, Wang B, Huang J, Yu G. Granular bamboo-derived activated carbon for high CO_2 adsorption: the dominant role of narrow micropores. ChemSusChem. 2012 Dec;5(12):2354-60.

[42] Sevilla M, Fuertes AB. Sustainable porous carbons with a superior performance for CO_2 capture. Energy & Environmental Science. 2011;4(5):1765-71.

[43] Li J, Michalkiewicz B, Min J, Ma C, Chen X, Gong J, Mijowska E, Tang T. Selective preparation of biomass-derived porous carbon with controllable pore sizes toward highly efficient CO_2 capture. Chemical Engineering Journal. 2019 Mar 15;360:250-9.

[44] Rashidi NA, Yusup S, Borhan A. Isotherm and thermodynamic analysis of carbon dioxide on activated carbon. Procedia engineering. 2016 Jan 1;148:630-7.

[45] Kovo AS. CO_2 capture using amine-impregnated activated carbon from jatropha curcas shell. British Journal of Applied Science & Technology. 2016 Jan 1;14(4):1.

[46] Rajahmundry GK, Garlapati C, Kumar PS, Alwi RS, Vo DV. Statistical analysis of adsorption isotherm models and its appropriate selection. Chemosphere. 2021 Aug 1;276:130176.

[47] Darvishi Cheshmeh Soltani R, Safari M, Rezaee A, Godini H. Application of a compound containing silica for removing ammonium in aqueous media. Environmental Progress & Sustainable Energy. 2015 Jan;34(1):105-11.

How to cite: Khoshraftar Z, Ghaemi A. Preparation of Activated Carbon from Entada Africana Guill. & Perr for CO_2 Capture: Artificial Neural Network and Isotherm Modeling. Journal of Chemical and Petroleum Engineering. 2022; 56(1): 165-180.

Appendix

The weights of the RBF network are presented in Table A1.

Table A1. The weights of RBF network with Levenberg-Marquardt algorithm

Neuron	1	2	3	4	5	6	7	8	9	10
IW{1,1}	-0.95205	-4.6498	-4.2967	-4.3362	-3.4764	-4.0559	-3.7245	1.1675	-2.4699	0.7053
	5.263	-0.65388	0.79438	-1.265	-3.5654	-0.59199	2.89	4.5297	-1.8386	-4.5716
b{1}	3.585	2.9496	2.56	1.1842	-0.26483	-0.79994	-1.1087	2.0934	-4.8113	4.2445
LW{2,1}	-1.6906	0.45472	-0.08057	-0.06529	-1.9462	-0.1839	-0.67141	-0.22446	-0.92397	-0.21734
b{2}	-1.1291									